Application of a distributed Shallow Landslide Analysis Model (dSLAM) to managed forested catchments in Oregon, USA

WEIMIN WU
Cacheva International Corporation, Santa Clara, California, USA

ROY C. SIDLE
LOICZ Core Project, Netherlands Institute for Sea Research, PO Box 59, 1790 AB Deb Burg-Texel, The Netherlands

Abstract A distributed, physically-based slope stability model (dSLAM) for analysing rapid, shallow landslides and the spatial distribution of the safety factor (FS) was tested in two catchments of the Cedar Creek watershed in the Oregon Coast Ranges. Simulated volumes and numbers of failures for a large storm in 1975 agreed closely with field measurements. The uncertainty associated with sensitive input parameters may complicate this comparison. For example, when soil cohesion values of 2.0 kPa and 3.0 kPa were used, the failure volume changed by factors of 2.04 and 0.41, respectively, for basin A, and 2.93 and 0.29, respectively, for basin B, compared with the standard condition of 2.5 kPa used in the simulation. Changes in values for soil depth and root cohesion that reflect potential natural variabilities, produced differences of up to several fold in simulated landslide volumes. As the simulated storm sequence progressed, FS declined sharply in hillslope hollows of basin A, the sites of most landslides. A similar response was noted in basin B, although the most unstable elements in this basin were associated with steep slopes. All areas with FS $<$ 2.0 were clearcut in 1968, 7 years prior to the storm.

INTRODUCTION

Most research on shallow landslides has focused on understanding temporal and on-site conditions and processes (Wu *et al.*, 1979; Sidle, 1992). To better understand the processes controlling landslides and to design appropriate land use strategies, it is necessary to evaluate slope stability and predict the occurrence of landslides in both temporal and spatial dimensions because of the distributed properties of site variables and land uses (Ward *et al.*, 1982; Carrara *et al.*, 1991).

When a distributed, physically-based approach is applied in basin slope stability analysis, not only are the distributed properties of site parameters of concern, but also the model output presents a spatial problem, because we need to determine the locations of slope failure. This is different from most runoff and erosion models which only predict outputs at basin outlets. Although geographic information system (GIS) technology is regarded as ideal tool for landslide analysis in terms of spatial data extraction and display (Carrara *et al.*, 1991), no progress has been reported in integrating distributed, physically-based slope stability modelling with GIS.

In this paper we discuss the application of dSLAM in two unstable forested basins in coastal Oregon subject to recent clearcutting. The effects of potential natural variabilities of input parameters on slope stability predictions are evaluated.

THEORETICAL BACKGROUND

The dSLAM model is a distributed, physically-based model that combines an infinite slope model, a kinematic wave groundwater model, and a continuous change vegetation root strength model to analyse shallow, rapid landslides and the spatial distribution of the factor of safety in steep forested terrain. The infinite slope model is modified to include the effects of vegetation root strength and tree weight as follows (Sidle, 1992)

$$FS = \frac{C + \Delta C + \{[(Z-h)\gamma_m + h\gamma_{sat} - h\gamma_w]\cos^2\beta + W\cos\beta\}\tan\phi}{[(Z-h)\gamma_m + h\gamma_{sat}]\sin\beta\cos\beta + W\sin\beta} \tag{1}$$

where C is the effective soil cohesion, ϕ is the effective internal friction angle, ΔC is the cohesion attributed to root strength, W is the vegetation surcharge, γ_m and γ_{sat} are the unit weights of soil at field moisture content and saturation, respectively, Z is the vertical soil thickness, h is the vertical height of the water table, β is the slope angle, and γ_w is the unit weight of water. In the application of dSLAM to steep forested areas, it is assumed that the infiltration capacity of the soil is always in excess of the rainfall intensity, thus only subsurface flow and non-Hortonian overland flow occur. Combined slope-parallel subsurface and saturated surface flows are routed by the kinematic wave model through topographically generated streamlines which lie orthogonal to the slope contours. For evaluating the continuous changes in vegetation root strength and surcharge following timber harvesting, Sidle's (1991, 1992) models are used. We assumed that all landslides are totally mobilized into debris flows. The extent of debris flow runout was based on channel gradient ($<3.5°$) and tributary junction angle ($>70°$) criteria (Wu & Sidle, 1995).

The dSLAM model is integrated with a contour line-based topographic analysis and a geographic information system (GIS) for spatial data extraction and display. Moore *et al.*'s (1988) TAPES-C model that subdivides an area into irregular polygons bounded by adjacent contour lines and adjacent streamlines is adopted. The GIS used in the study is the ARC/INFO system.

SITE CONDITIONS

The dSLAM model was tested in two second-order basins (A=1.18 km^2 and B=1.12 km^2) within the Cedar Creek watershed in the Oregon Coast Ranges in which both the temporal and spatial patterns of timber harvesting were known and different. The study basins have relatively shallow mantles of permeable, low-cohesion soils overlying sandstone bedrock. Forest cover consists of Douglas-fir with small pockets of red alder. Other site details are given by Wu & Sidle (1995).

From the early 1950*s* through to the late 1960*s* timber harvesting and development of logging roads increased in this area. Because the slopes are very steep and the soil strength is very low, periods of heavy rainfall often trigger landslides. A series of high intensity storms in the mid-1970*s* triggered a large number of landslides in the area, both from roads and within clearcuts.

METHODOLOGY

The 7.5' USGS digital elevation model (DEM) of Goodwin Peak Quadrangle was used to derive the vector DEM input for the TAPES-C model, a topographic analysis program developed by Moore *et al.* (1988). Once the vector DEM was generated, it was used by TAPES-C to derive the contour line-based network and to calculate topographic attributes. The network was then used as a framework for generation of other distributed information and visualization of results. Details of the operational procedures and discussion of DEM accuracy are given by Wu & Sidle (1995). There are 13 595 elements (average element size = 82.4 m^2) and 66 contours in basin B. In basin A, the average element size is 100.5 m^2 with 52 contours and 11 764 elements.

The spatial data for soil and vegetation were extracted from a GIS maintained by the Siuslaw National Forest. Past harvesting patterns and the spatial distribution of different soil types are documented by Wu (1993). Soil depths and saturated hydraulic conductivities (k_{sat}) used in simulations were 1.0-1.5 m and 0.5-1.0 m h^{-1}, respectively. Soil engineering properties, root cohesion, and vegetation surcharge are documented by Wu & Sidle (1995).

Heads of perennial channels were defined as having a contributing area of at least 2500 m^2 based on nearby studies (Montgomery & Dietrich, 1988). No adequate method was found to assess FS for channelized elements, and they were therefore excluded from the slope stability analysis. Most channels in this area are eroded to bedrock, thus this assumption seemed reasonable.

A major rainstorm in late November of 1975 that caused widespread landsliding near Cedar Creek was chosen for the simulation. Antecedent moisture conditions were relatively wet (18 mm of rain in the 24 h preceding the storm). Three landslides with a total volume of 734 m^3 occurred in basin A and six landslides (total volume=749 m^3) occurred in basin B according to a post-storm survey (Greswell *et al.*, 1979).

RESULTS OF SLOPE STABILITY SIMULATIONS

During the 1975 rainstorm, a total landslide volume of 733 m^3 was simulated in basin A. These four landslides occurred on steep slopes (36.5 to 47.9°) that were clearcut in 1968. The three landslides in the eastern portion of the basin converged into a single debris flow. A debris flow initiating further to the west joined this debris flow at the channel junction. The combined debris flow produced by these two source areas was deposited near the outlet of basin A due to the gentle channel gradient in that reach (see Wu & Sidle, 1995).

In basin B, seven discrete landslides were simulated with a total volume of 801 m^3. Slope gradients of failed elements in basin B ranged from 38.4 to 45.1°. Again, all landslides occurred in areas harvested in 1968. The seven landslides occurred close together in the same tributary and the total volume of these failures moved out of the basin as a debris flow.

The simulated landslide volumes and the numbers of landslides are very close to the inventory data from the 1975 landslide survey: 734 m^3 and 3, in basin A, and

749 m^3 and 6, in basin B. One more landslide was simulated in each basin than actually occurred during the 1975 storm. However, the scale of resolution for separating individual landslides both in the simulations and in the field surveys negates this small difference. The locations of the failed elements are reasonable, although it appears that the sites of landslides in basin A are more consistent with sites where groundwater flow converges; in basin B, some failure sites are more related to steep slopes.

Spatial and temporal changes in FS for basin B during the November 1975 storm are shown in Fig. 1. The temporal sequence (0, 22, and 62 h from the beginning of the storm) represents pre-storm, end of storm, and post-storm FS distributions. Similar data for basin A are presented by Wu & Sidle (1995). In both basins, pre-storm patterns of FS were largely controlled by slope gradient and timber harvesting patterns. The most unstable sites corresponded to areas clearcut in 1968, 7 years prior to the storm. This timing corresponds to the predicted minimum in net root cohesion following timber harvest and subsequent regrowth (Sidle, 1991). During the rainstorm, areas with low FS values (1.0-1.6) expanded dramatically and after rainfall ceased, these areas slowly decreased in size. Prior to the storm, channel heads were relatively stable in both basins, however, as rainfall progressed FS declined sharply in the vicinity of these areas. This rapid decline is more apparent in basin A than in basin B. The location of the most unstable elements in basin B appear to be more related to steep slopes (Fig. 1) rather than to the unstable head hollow sites which appeared to be the primary initiation zones in basin A.

EFFECTS OF PARAMETER UNCERTAINTY ON SLOPE STABILITY

Even though dSLAM closely predicted numbers and volumes of landslides during the simulated 1975 storm, we need to test the sensitivity of the model to variations in input parameters for reasonable ranges that may occur in the field. Although some of the input data were spatially distributed (e.g. soil depth, vegetation, timber harvesting patterns), other data (e.g. soil engineering properties) were averaged over the entire basin due to lack of spatially distributed data. Furthermore, many data that were available in a spatially distributed form did not adequately represent the desired degree of resolution for this type of analysis.

Changes in soil cohesion in the range reported by Schroeder & Alto (1983) for the area had the greatest effect on FS of all parameters tested (Fig. 2). When the highest value of C (6.86 kPa) was used, no landslides occurred in either basin. However, when cohesion was reduced to 0 kPa, failure volume increased 29- and 85-fold in basins A and B, respectively, above the volumes obtained when the average cohesion value (2.5 kPa) was used in the simulations (Fig. 2). If soil cohesion is decreased from 2.5 kPa to 0 kPa, more land area in basin A becomes marginally stable than in basin B. If C values of 2.0 and 3.0 kPa are used, the failure volume changes by factors of 2.04 and 0.41, respectively, for basin A and 2.93 and 0.29, respectively, for basin B compared with the standard condition. These are quite large variations (up to 10-fold differences in basin B) in failure prediction for relatively small changes (± 0.5 kPa) in input values of C.

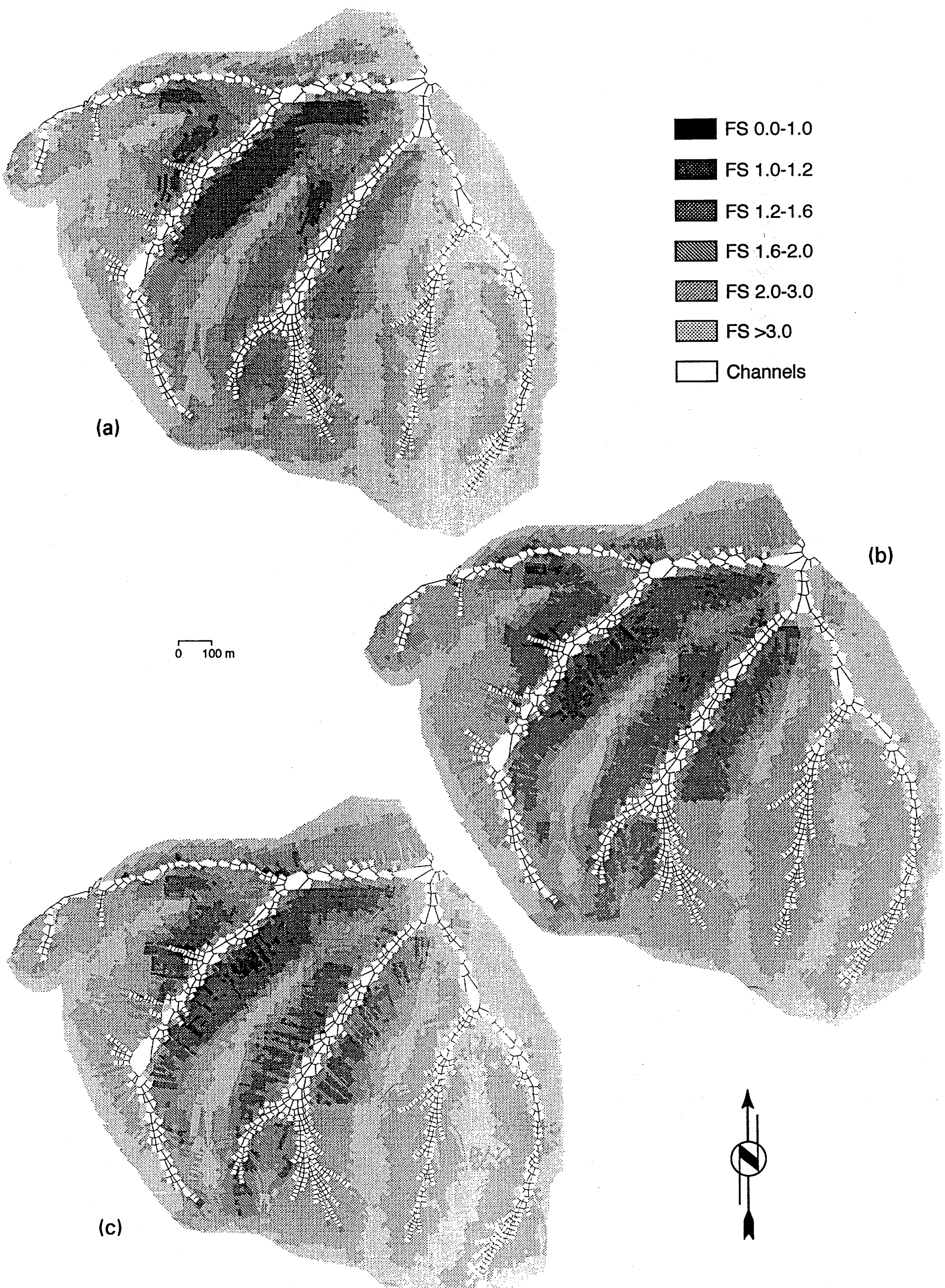

Fig. 1 The spatial distribution of FS simulated for the 1975 winter storm in basin B: (a), at 0 h (before the storm); (b) at 22 h (at the end of the storm); (c) at 62 h (40 h after the storm).

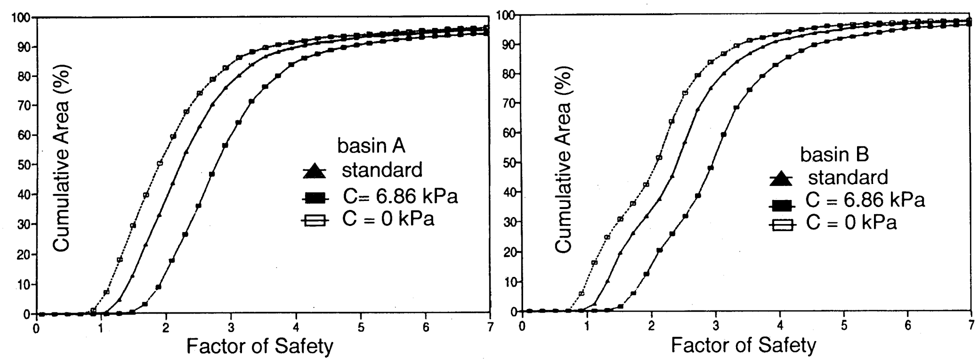

Fig. 2 The effects of changes in soil cohesion on slope stability in basins A and B.

To estimate the effect of natural variability of soil depth within soil mapping units on FS, soil depth was increased and decreased by 30% with respect to the average soil depth assumed for each unit. Failure volumes for the 30% increase in soil depth increased by factors of 2.0 and 3.9 (compared with average depth) in basins A and B, respectively; for the 30% decrease, failure volumes declined by factors of 0.27 and 0.06 in these respective basins (Fig. 3). The greater response in FS observed in basin B is likely to be due to the steeper slopes.

For the internal friction angle, the relative range of data (35.3°-41.4°) is smaller than that of soil cohesion and the effect of this variation on FS is much smaller (Fig. 4). Using the maximum value of 41.4°, failure volumes change by factors of 0.32 for basin A and 0.35 for basin B; and 2.25 and 2.64, respectively, for the minimum value of 35.3°. The relative temporal and spatial response of FS in basin A was similar to that in basin B for similar changes in internal friction angle. It appears that the natural variability in internal friction angle within these basins would not produce large deviations from FS calculated based on average values.

Changes in k_{sat} affected FS only slightly compared to other variables, possibly due to the relatively high k_{sat} values of these forest soils. The timing of failure, however, is slightly affected: landslides occur earlier during the storm for larger values of k_{sat}.

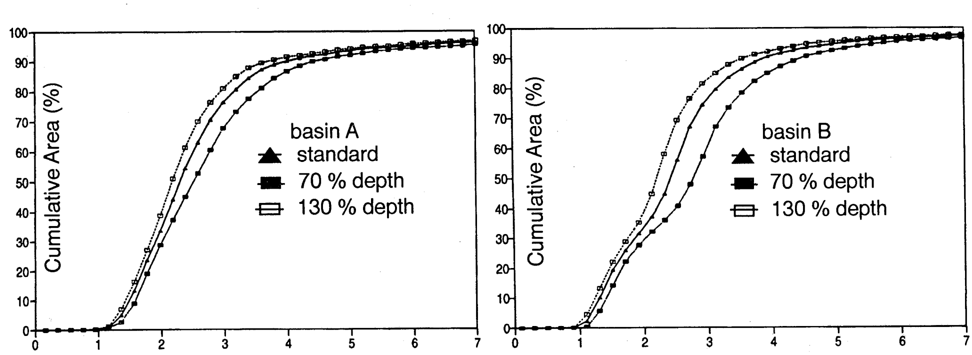

Fig. 3 The effects of a 30% increase and decrease in soil depth on slope stability in basins A and B.

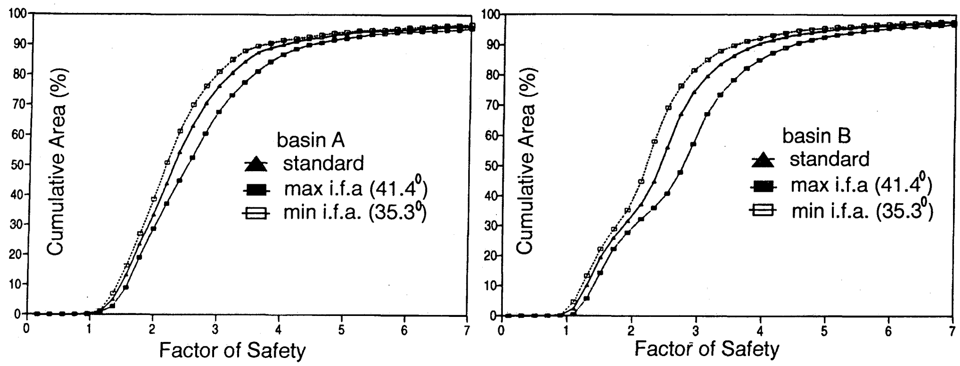

Fig. 4 The effects of changes in internal friction angle on slope stability in basins A and B.

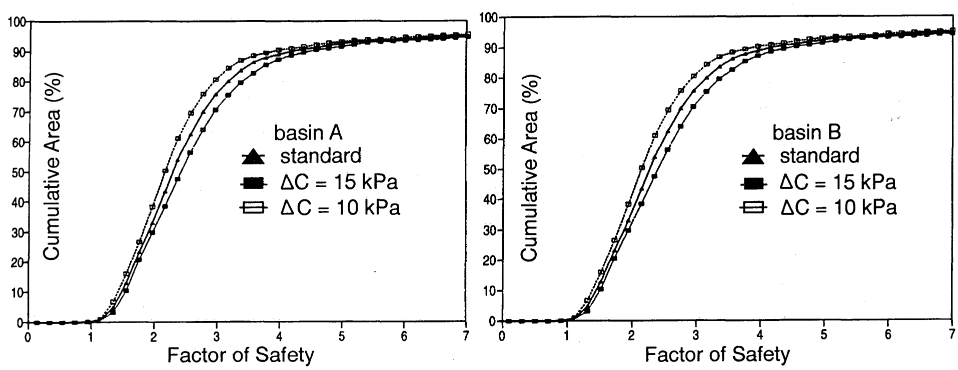

Fig. 5 The effects of ± 2.5 kPa changes in maximum root cohesion on slope stability in basins A and B.

When the porosity changes from 0.37 (standard condition) to 0.30, failure volumes increase by 3.13- and 4.05-fold in basins A and B, respectively. For a porosity of 0.40, failure volumes in basins A and B decrease by factors of 0.66 and 0.61, respectively. However, the changes in the cumulative area-FS distributions are small.

If the maximum root cohesion changes from 12.5 kPa to 10 kPa, failure volumes increase by 1.73 and 2.65-fold for basins A and B, respectively. For the case of $\Delta C = 15$ kPa, failure volumes decrease by factors of 0.55 and 0.29, respectively. Figure 5 shows the changes of FS distribution due to a 20% change in maximum root strength from the standard condition. The widest spread in FS values between the two ΔC extremes (10 and 15 kPa) occurs in the FS range from 2.0 to 3.5. Even though FS decreases in this range did not contribute to landsliding for this storm simulation, they could affect landsliding in larger storms.

Figure 6 shows the effect of: (a) changing the root strength regrowth inflection point (t_i) for Douglas-fir (18 to 25 years) and alder (15 to 20 years) and (b) changing the root decay curve constant (n) from 0.73 to 0.70. In the first case, failure volumes increased 1.56-fold (basin A) and 1.82-fold (basin B) compared with standard conditions. Thus, slower regrowth of regenerating trees can significantly increase landslide potential in steep forested terrain. In the second case (decreasing n), failure

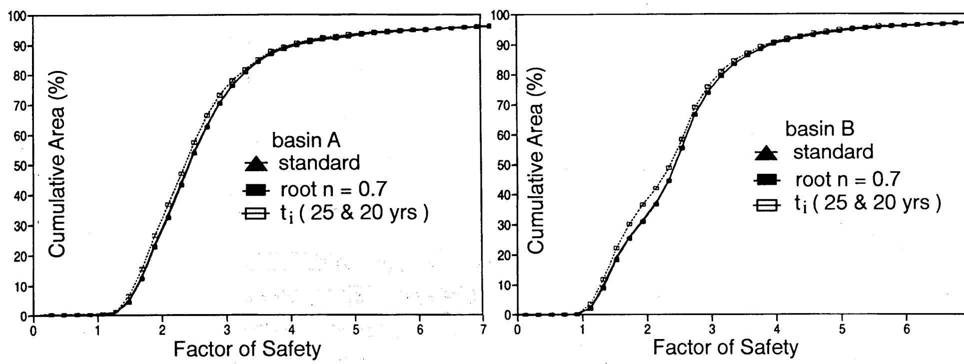

Fig. 6 The effects of increases in the root strength regrowth inflection point (from 18 to 25 years for Douglas-fir and from 15 to 20 years for alder) and decreases in root decay curve constant: (*n* from 0.73 to 0.70) on slope stability in basins A and B (see Sidle, 1991 for description of constants).

volume was unchanged in basin A and decreased by a factor of 0.82 in basin B compared with standard conditions.

When the threshold contributing area for propagation of a stream channel is reduced to 1000 m^2, no failures occur in basin A and failure volume is drastically reduced (by a factor of 0.05) in basin B. By increasing the threshold contributing area to 5000 m^2, failure volumes increase 3.12- and 1.38-fold in basins A and B, respectively.

To determine the effect of different distributions of rainfall hyetographs, the sequence of intensity of the 1975 winter storm was rearranged with the duration and rainfall volume unchanged. If the hyetograph is reversed, failure volume increases by a factor of 1.13 in basin A and is unchanged in basin B. There is no change in failure volume if a normal distribution is used.

For the case of 5% initial saturation (by depth) of the soil profile (0% for standard condition), failure volumes increase by 1.62- and 1.92-fold, respectively, for basins A and B. However, changes in FS distributions throughout other portions of the basins were small.

Even though the stability simulations indicate that FS is largely controlled by topography, slope gradient, timber harvesting, and groundwater flow patterns, the influence of natural variabilities in soil depth, soil cohesion, and other soil properties are apparent.

REFERENCES

Carrara, A., Cardinal, M., Detti, R., Guzzetti, F., Pasqui, V. & Reichenbach, P. (1991) GIS techniques and statistical models in evaluating landslide hazard. *Earth Surf. Processes and Landforms* **16**, 427-445.

Greswell, S., Heller, D. & Swanston, D. N. (1979) Mass movement response to forest management in the central Oregon Coast Range. *USDA Forest Service Res. Bull.* **PNW-84**. Pacific N.W. Res. Stn., Juneau, Alaska.

Montgomery, D. R. & Dietrich, W. E. (1988) Where do channels begin? *Nature* **336**(17), 232-234.

Moore, I. D., O'Loughlin, E. M. & Burch, G. J. (1988) A contour based topographic model and its hydrologic and ecological applications. *Earth Surf. Processes and Landforms* **13**, 305-320.

Scheroeder, W. L. & Alto, J.V. (1983) Soil properties for slope stability analysis; Oregon and Washington coastal mountains. *Forest Sci.* **29**, 823-833.

Sidle, R. C. (1991) A conceptual model of changes in root cohesion in response to vegetation management. *J. Environ. Qual.* **20**, 43-52.

Sidle, R. C. (1992) A theoretical model of the effects of timber harvesting on slope stability. *Wat. Resour. Res.* **28**, 1897-1910.

Ward, T. J., Li, R. & Simons, D. B. (1982) Mapping landslide hazards in forest watersheds. *J. Geotech. Engng Div. ASCE* **108**(GT2), 319-324.

Wu, W. (1993) Distributed slope stability analysis in steep forested basins. PhD Dissertation, Utah State University, Logan.

Wu, T. H., McKinnel, W. P. & Swanston, D. N. (1979) Strength of tree roots and landslides on Prince of Wales Island, Alaska. *Can. Geotech. J.* **16**, 19-33.

Wu, W. & Sidle, R. C. (1995) A distributed slope stability model for steep forested basins. *Wat. Resour. Res.* **31**, 2097-2110.